Density Functional Study of the Phase Diagram and Pressure-Induced Superconductivity in P: Implication for Spintronics

S. Ostanin,[1] V. Trubitsin,[2] J. B. Staunton,[1] and S. Y. Savrasov[3]

[1]*Department of Physics, University of Warwick, Coventry CV4 7AL, United Kingdom*
[2]*Physico-Technical Institute, Ural Branch of RAS, 132 Kirov Street, 426001 Izhevsk, Russia*
[3]*Department of Physics, New Jersey Institute of Technology, Newark, New Jersey 07102, USA*
(Received 21 January 2003; published 22 August 2003)

The high-pressure phase diagram of *P* is studied using density functional total energy, linear response lattice dynamics and model Debye-Grüneisen theories. The volume dependent electron-phonon coupling $\lambda \sim 0.7$–0.9 is extracted for the bcc structure and found to increase with increasing volume. We propose that this phase might be realized in epitaxial thin films using templates such as V(100), Fe(100), or Cr(100) relevant to spintronics applications.

The study of properties of materials under pressure is a key experimental technique and recent discoveries of superconductivity in such simple metals as compressed Fe [1] and Li [2] are currently generating enormous interest [3–5]. Black insulating phosphorus, with an orthorhombic A17 structure, which is the most stable form at ambient conditions, exhibits a series of pressure-induced phase transitions [6–9]. The first is a transformation to a metallic phase with simple cubic structure at 10 GPa. This phase is known to superconduct with $T_c = 10$ K [9]. An observation of a new simple bcc structure above 262 GPa has been made recently [7], which points out that similar or even stronger electron-phonon interaction and pressure-induced superconductivity may be also realized in bcc P. Growth of P containing materials by thin film techniques has been developed very recently [10] to fabricate the class of wide gap phosphide ferromagnetic semiconductors which may provide an ideal opportunity to stabilize the bcc phase of P at ambient conditions using suitable templates such as the V(100), Fe(100), or Cr(100) substrates. This may lead to a significant breakthrough in technological spintronics applications in which combined spin and superconducting degrees of freedom will provide a new level of functionality for microelectronic devices.

In this Letter we address both the issue of the phase stability of P as well as the superconductivity of its highly pressurized bcc structure. We use *ab initio* density functional total energy [11] and linear response [12] techniques which have proven to provide a reliable description of various ground state properties for a large class of materials. We also study the electronic structure of the $Fe_5/P_n/Fe_4$ ($n = 3, 5$) superlattices to investigate the problem of how to stabilize the bcc phase under ambient pressure conditions.

In the past, structural phase transformations in P have been the subject of many experimental [6–9] and theoretical [13–15] density functional theory (DFT) based studies. Orthorhombic A17 structured P transforms to the rhombohedral A7 phase at 4.5 GPa [6]. This A7 phase, which is similar to the structure of such group-V elements as As, Sb, and Bi, undergoes a transition to the simple cubic (sc) metallic phase at 10 GPa [6]. With increasing pressure, at 137 GPa, the sc structure transforms into a simple hexagonal (sh) one [7]. This sc $\rightarrow$ sh transition, which is accompanied by a large volume reduction of 7.6%, is the first such observation reported for an elemental system. Since the sh structure has a low atomic packing fraction, namely, 0.605, a phase with a higher packing fraction such as bcc, fcc or hcp is expected at higher pressures. Indeed, with increasing pressure, the c/a ratio of the sh phase increases from 0.948 to 0.956, and, finally, above 262 GPa, a new high-pressure phase is observed, which has been proposed to be bcc [7]. A high-pressure bcc structure has also been found in Sb at 28 GPa and in Bi at 7.7 GPa [16], but, in contrast, the sh phase of Si and Ge transforms to the hcp structure [17].

To date, no full theoretical description of the phase stability in P under extreme high pressure has been reported. Using the pseudopotential method, Chang and Cohen [13] reproduced the A17 $\rightarrow$ A7 $\rightarrow$ sc phase transitions, with the crystal energy of the A7 phase being shifted by 2.3 mRy, but failed to find any stable closed-packed P phase at high pressure. In contrast, Sasaki *et al.* [14] inferred a sc $\rightarrow$ bcc transition at a pressure of 135 GPa, rather far from the recent experimental observations [7]. In this work we emphasize the role of phonons in the phase diagram of P and show that simultaneous electronic structure and lattice dynamics calculations can successfully describe all high-pressure transitions and, in particular, quantify the sh-bcc transition, the highest-pressure structural transformation observed up to now for an elemental material.

To predict the sequence of sc $\rightarrow$ sh $\rightarrow$ bcc transitions, we first carry out highly precise calculations of the total electronic energy versus volume, $E(V)$, behavior using the full potential linearized augmented plane waves (LAPW) method of the Wien group [18], which is one

of the most accurate DFT schemes. The theoretical equations of state, $P(V) = -\partial E/\partial V$, have been extracted numerically from the calculated $E(V)$ data. Then, the thermodynamical Gibbs potential $G(P) = E(V) + PV$ is analyzed as a function of pressure. The results of these calculations produce theoretical transition pressures which we find in quite good agreement with experiment: the sc $\rightarrow$ sh transition is predicted at 120 GPa (experimental value is 137 GPa [7]) while the sh $\rightarrow$ bcc transition is predicted at 258 GPa (experimental value is 262 GPa [7]). From the calculated equations of states we can estimate the equilibrium atomic volume of the bcc structure at the transition point $V_{bcc} = 7.15$ Å^3 which is in very good agreement with the value 7.1 Å^3 determined experimentally [7]. We also predict a volume collapse of about 3% at the transition point consistent with what is seen from the experimental equation of state in Ref. [7]. The calculated volume collapse at sc $\rightarrow$ sh transition is about 10% which is a little larger than the measured value of 7.6% [7].

To reconstruct the full pressure-temperature phase diagram seen directly by experiment, these calculations should be supplemented with the analysis of the phonon free energy $F^{ph}(V, T)$ which will deliver the total Gibbs potential. (While the electronic entropy term should also be included in this analysis, at least in principle, owing to the absence of strong electron correlation effects and the temperature range this contribution is believed to be small and is neglected in the present study.) The use of the Debye-Grüneisen theory is the simplest way to account for the phonon counterpart, by using the volume dependent characteristic Debye temperature $\Theta_D(V)$ for each phase. A more sophisticated approach is to use linear response theory [19] to compute the entire phonon dispersions $\omega_\nu(\mathbf{q})$ at different volumes and perform precise free energy estimates.

For our study, we utilize both of these methods. We first use a linear muffin-tin orbital (LMTO) based linear response method [19] which has proven to describe accurately the phonon dispersions of various systems [20,21] including studies at high pressures [22]. The dispersion relations $\omega_\nu(\mathbf{q})$ have been calculated for bcc P at three representative lattice constants corresponding to volumes $V_1 = 7.1$ Å^3, $V_2 = 9.2$ Å^3, $V_3 = 11.8$ Å^3. The results of these calculations are shown at Fig. 1, where blue, green, and red lines corresponds to the volumes V_1, V_2, and V_3, respectively. We see that the phonons show a remarkable hardening as the volume decreases. The structural instability can be seen for the volume V_3 in the transverse branch T' along $(0\xi\xi)$. At this volume, however, phosphorus does not crystallize in the bcc phase and our theoretical calculation is purely hypothetical. The appearance of this unstable mode poses a challenge for the proper evaluation of phonon free energy. Fortunately, we are able to estimate $F^{ph}(V, T)$ without this problem for two lattice constants, where the stable lattice dynam-
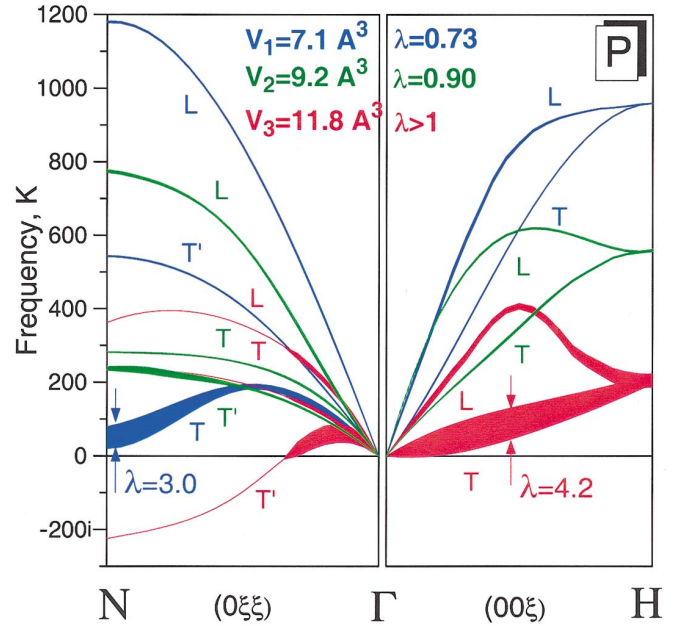

FIG. 1 (color). Phonon dispersions of bcc P at the three different volumes. The curves are widened proportionally to electron-phonon coupling at each $\omega(\mathbf{q})$. The structural instability for volume V_3 along $(0\xi\xi)$ is shown by the imaginary frequency branch reaching the value of 220i at $\mathbf{q} = (011)$.

ics emerges. We can compare these calculations with the results of the Debye-Grüneisen theory, where the $\Theta_D(V)$ is obtained from the knowledge of the bulk modulus B, the atomic mass of phosphorus, m_P, and its lattice constant a, i.e., $\Theta_D(V) = c(aB/m_P)^{1/2}$. Here c is the universal coefficient calculated for bcc lattices many years ago [23]. We conclude that both the two approaches compare well with each other while the typical discrepancy in determination of the free energy from the model is of the order of 200 K. The successful applicability of this model has been also demonstrated [24] recently for several other materials under pressure.

Using the simplified Debye-Grüneisen approach, we perform further similar calculations of $\Theta_D(V)$ in two other (sc and sh) structures. These data now allow us to find corrected transition pressures as functions of temperature. For example, at $T = 0$, the transition pressures become: $P_{sc\rightarrow sh} = 123$ GPa, and $P_{sh\rightarrow bcc} = 246$ GPa. Interestingly, the corrections due to phonons are of the order of 3–12 GPa, which are in principle not so small from the experimental point of view. Finally, Fig. 2 shows the fully reconstructed (P, T) phase diagram where two experimental points indicated by symbols are lying close to the theoretical lines.

The recent discovery of superconductivity in the sc phase of P below 10 K [9] produces the assumption of a relatively strong electron-phonon interaction. Similar or even stronger coupling may also be realized in bcc P. We investigate this possibility by using our calculated phonon dispersions at various volumes, and extracting
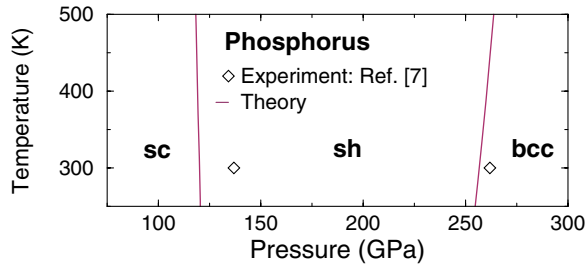
FIG. 2 (color online). Pressure-temperature phase diagram of P calculated in this work. Symbols show experimental points from Ref. [7].

the $\mathbf{q}$-dependent coupling constant $\lambda_\nu(\mathbf{q})$ for each phonon branch using the approach developed earlier [20]. The results of our calculations are shown on Fig. 1 by widening the dispersions $\omega_\nu(\mathbf{q})$ proportionally to $\lambda_\nu(\mathbf{q})$ at each point. We indeed find remarkably large coupling constants at $\mathbf{q}$ points where the widening is seen to be largest. For example, the calculated $\lambda_\nu(\mathbf{q}) \sim 4$ is found within a soft transverse branch T along (00ξ) at the volume V_3 (red line). The calculated $\lambda_\nu(\mathbf{q}) \sim 3$ is found within a nearly unstable transverse branch T along $(0\xi\xi)$ at V_1 (blue line). The appearance of large λ near the instability can be understood by utilizing the formula $\lambda(\mathbf{q}) \sim \eta(\mathbf{q})/\Lambda(\mathbf{q})$, where the so-called Hopfield parameter $\eta(\mathbf{q})$ is roughly proportional to the absolute square of the electron-phonon scattering matrix element $g(\mathbf{q})$ and the density of states at the Fermi level $N(0)$, i.e., $\eta(\mathbf{q}) \sim N(0)|g(\mathbf{q})|^2$. If the force constant $\Lambda(\mathbf{q})$ for a given mode becomes small, this may result in a large $\lambda(\mathbf{q})$. Importantly, we have also found relatively large λ's of the order of 1 for another branch T' along the $(0\xi\xi)$ direction at the volume V_2, which are fairly stable. Our total estimated $\lambda_1 = 0.73$ and $\lambda_2 = 0.90$. For the volume V_3 the calculation is complicated due the presence of imaginary frequencies, but even neglecting the unstable modes completely, the value of λ_3 comes out to be about 3. This is mainly due to anomalously large λ's seen from the fat red T line along (00ξ). We therefore reach the conclusion that while the bcc phase is found experimentally only for volumes smaller than V_1, expanding this lattice may in fact increase greatly the strength of the electron-phonon coupling.

The analogy with aluminum can be discussed which has a p band filled with one electron. It is known that Al has a superconducting $T_c \sim 1$ K and coupling constant $\lambda \sim 0.4$ [20]. We find that the value of the density of states at the Fermi level in P does not differ significantly from the one known in Al, equal to 0.4 states/[eV atom]. Why is the coupling in bcc P at least twice as much? This is mainly due to two reasons: (i) the appearance of soft phonons seen from Fig. 1, and, (ii), the proximity of the $3d$ band to the Fermi level, which already crosses it at the pressures corresponding to V_1. The latter results in significantly larger electron-phonon matrix elements $g_{pd}(\mathbf{q})$ in the $p \to d$ scattering channel, and has this impact upon λ.

The estimate of the superconducting transition temperature is a more challenging question due to the appearance of the unknown Coulomb pseudopotential μ^* in the Eliashberg theory of superconductivity. We assume the same value for $\mu^* \sim 0.1$ as for Al [25]. The same choice of $\mu^* \sim 0.1$ is consistent with estimates [15] which reproduce the experimentally known $T_c \sim 10$ K of sc-P at $V_{sc} = 12.6$ Å^3 using $\lambda \sim 0.7$, $\mu^* \sim 0.1$, and $\omega_{\log} \sim 300$ K ($\omega_D \sim 410$ K). Utilizing the Allen-Dynes modified McMillan expression [26] for T_c we obtain the values 14 and 22 K for the solutions at volumes V_1 and V_2 using the logarithmically averaged phonon frequencies $\omega_{\log}$ to be equal to 375 and 370 K, respectively. These have been determined from the Eliashberg spectral function $\alpha^2 F(\omega)$, and their closeness reflects the fact that the coupling is mainly due to low-frequency branches. We also find from the phonon densities of states that the average frequencies $\bar{\omega}$ are significantly higher, substantially different, and equal to 670 and 440 K for V_1 and V_2 correspondingly. We finally speculate on the tendency for increased T_c of the solution at V_3 due to the possible sharp increase in λ which may compensate further lowering of $\langle\omega\rangle$.

The expected increase in T_c poses a question on stabilizing the bcc structure at larger volumes. Epitaxial thin film structures may offer ideal opportunities to create an expanded lattice at ambient conditions using suitable growth templates such as the V(100), Fe(100), or Cr(100) substrates. Moreover, there is considerable current interest in technological spintronics applications, in which the spin of carriers is exploited to provide new functionality for microelectronic devices. Growth of P containing materials by thin film techniques, such as molecular beam epitaxy or pulsed laser deposition, has been developed to fabricate the class of wide gap phosphide ferromagnetic semiconductors [10]. Consequently, we now turn to study the electronic and magnetic properties of thin films of P (3–5 layers in thickness) embedded in ferromagnetic bcc-Fe. Despite the considerable theoretical and experimental progress that has been made during the last decade towards understanding metallic magnetism in superlattices and multilayers, no such investigation has been made for Fe/P until now.

The electronic structure of the $Fe_5/P_n/Fe_4$ ($n = 3, 5$) superlattices, is calculated with the lattice constant of bulk Fe. Figure 3 shows the total and layer-resolved electronic density of states (DOS) for $n = 3$. Evidently the DOS of phosphorus is fairly insensitive to monolayer (ML) position and p-d hybridization has broadened d-related peaks in the Fe interface DOS. Figure 4 shows the layer-resolved spin magnetic moments and the spin magnetic moment per atom on the Fe interface layer to be about 20% smaller than that of bulk bcc-Fe whereas the second Fe layer from the ideally sharp Fe/P interface has an enhanced local spin moment compared to that of bulk Fe. The P atoms distant from the interface have no induced magnetic moments. The spin magnetic moment on
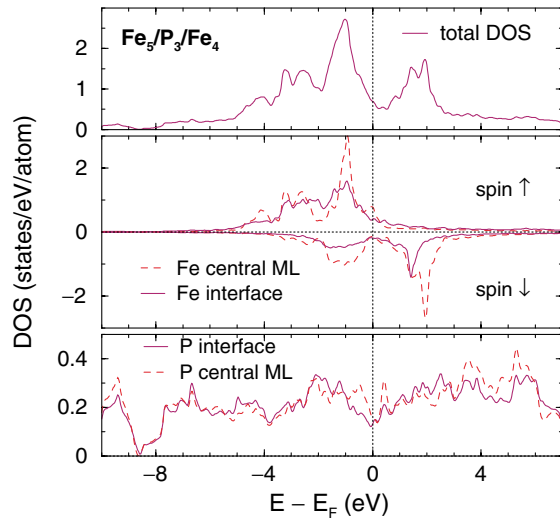
FIG. 3 (color online). Total and layer-resolved electronic DOS of the $Fe_5/P_3/Fe_4$ superlattices with the lattice constant of bulk Fe.

FIG. 4. Layer-resolved spin moments of Fe and P in the $Fe_5/P_3/Fe_4$ superlattices with the lattice constant of bulk Fe.

the P interface atoms are tiny and antiparallel to the Fe magnetization direction.

Thus, the total magnetic moments of the Fe/P/Fe superlattices, which are almost independent of the thickness of P, are slightly reduced from those of a relevant pure Fe system due to the antiferromangetic Fe-P interface coupling. Obviously, this effect would be important for superlattices with thin Fe slabs. We note that a similar but more pronounced antiferromagnetic coupling takes place at the Fe/V (001) interface [27,28].

The proximity effect in the ferromagnet/ superconductor heterostructures means that the Cooper pair amplitude in an exchange field does not decay exponentially to zero on the FM side but oscillates with decreasing amplitude as a function of the distance from the interface. These oscillations occurring in what is known as the Fulde-Ferrell-Larkin-Ovchinnikov state [29] may lead to striking changes in the transition temperature (as observed in Fe/V and Fe/Nb heterostructures [30]) as a function of the ferromagnetic slab thickness d_{Fe}. We suggest that Fe/P heterostructures may show similar effects.

Another interesting application of the superconducting state in the stabilized bcc phase of P might be available with V/Fe/P junctions, in which thin ferromagnetic films are sandwiched between two superconductors with different transition temperatures. Such systems support spontaneous currents parallel to the ferromagnet/superconductor interface while the spin polarization of these currents depends on band filling [31] and, hence, can be readily adjusted.

In summary, our high-pressure study of P, based upon DFT total energy, linear response lattice dynamics, and Debye-Grüneisen model calculations, produc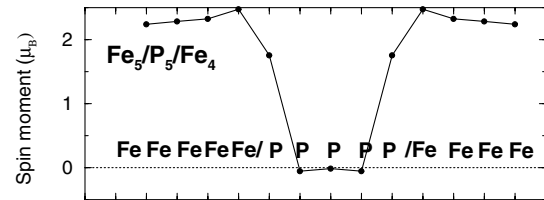es a pressure-temperature phase diagram in good agreement with experiment. Pressure-induced superconductivity is predicted for the bcc phase, and its realization with potentially a large T_c can be expected in Fe/P hetero-structures relevant to spintronics applications.

[1] K. Shimizu *et al.*, Nature (London) **412**, 316 (2001).
[2] K. Shimizu *et al.*, Nature (London) **419**, 597 (2002).
[3] N. W. Ashcroft, Nature (London) **419**, 569 (2002).
[4] I. I. Mazin *et al.*, Phys. Rev. B **65**, 100511 (2002).
[5] S. K. Bose *et al.*, cond-mat/0207318.
[6] T. Kikegawa *et al.*, Acta Crystallogr. Sect. B **39**, 158 (1983).
[7] Y. Akahama *et al.*, Phys. Rev. B **61**, 3139 (2000).
[8] Y. Akahama *et al.*, Phys. Rev. B **59**, 8520 (1999).
[9] H. Kawamura *et al.*, Solid State Commun. **49**, 879 (1984); **54**, 775 (1985).
[10] S. J. Pearton *et al.*, Appl. Phys. **93**, 1 (2003).
[11] For a review, see, e.g., *Theory of the Inhomogeneous Electron Gas*, edited by S. Lundqvist and S. H. March (Plenum, New York, 1983).
[12] S. Baroni *et al.*, Rev. Mod. Phys. **73**, 515–563 (2001).
[13] K. J. Chang *et al.*, Phys. Rev. B **33**, 6177 (1986).
[14] T. Sasaki *et al.*, J. Phys. Soc. Jpn. **57**, 978 (1988).
[15] M. Rajagopalan *et al.*, J. Low Temp. Phys. **75**, 1 (1989).
[16] K. K. Aoki *et al.*, Solid State Commun. **45**, 161 (1983); J. Phys. Soc. Jpn. **51**, 3826 (1982).
[17] Y. K. Vohra *et al.*, Phys. Rev. Lett. **56**, 1944 (1986).
[18] P. Blaha *et al.*, Comput. Phys. Commun. **59**, 399 (1990).
[19] S. Y. Savrasov, Phys. Rev. Lett. **69**, 2819 (1992).
[20] S. Y. Savrasov *et al.*, Phys. Rev. Lett. **72**, 372 (1994).
[21] Y. Kong *et al.*, Phys. Rev. B **64**, 020501 (2001).
[22] S. Ostanin *et al.*, Comput. Mater. Sci. **17**, 202 (2000).
[23] V. L. Moruzzi *et al.*, Phys. Rev. B **37**, 790 (1988).
[24] S. A. Ostanin *et al.*, Phys. Rev. B **57**, 13 485 (1998).
[25] K. H. Lee *et al.*, Phys. Rev. B **52**, 1425 (1995).
[26] P. B. Allen *et al.*, Phys. Rev. B **12**, 905 (1975).
[27] B. Hjörvarsson *et al.*, Phys. Rev. Lett. **79**, 901 (1997).
[28] S. Ostanin *et al.*, Phys. Rev. B **61**, 4870 (2000).
[29] P. Fulde *et al.*, Phys. Rev. **135**, A550 (1964); A. Larkin *et al.*, Sov. Phys. JETP **20**, 762 (1965).
[30] H. K. Wong *et al.*, J. Low Temp. Phys. **63**, 307 (1986).
[31] M. Krawiec *et al.*, Phys. Rev. B **66**, 172505 (2002).